Available online at www.sciencedirect.com
ScienceDirect
Journal of Power Sources 173 (2007) 367–374
JOURNAL OF POWER SOURCES
www.elsevier.com/locate/jpowsour

Concentration and ohmic losses in free-breathing PEMFC

Luis Matamoros *, Dieter Brüggemann

Lehrstuhl für Technische Thermodynamik und Transportprozesse, Universität Bayreuth, 95440 Bayreuth, Germany

Received 17 August 2006; received in revised form 23 January 2007; accepted 24 February 2007
Available online 25 April 2007

Abstract

Non-isothermal and three-dimensional simulations were carried out to study concentration and ohmic losses in free-breathing PEMFC under diverse conditions. Flow fields, species transport, transport of water in polymer membrane and movement of liquid water in cathode and anode porous layers were determined. Numerical results were obtained under different hydrating conditions, cell temperatures, cathode catalyst loadings and channel lengths. Current density and polymer electrolyte water content distributions as well as average power density were used as main output variables to study effects of operative conditions on performance. Results show that slow oxygen transport to active sites constitutes the most limiting factor to consider. Dehydrating conditions slightly affect free-breathing PEMFC performance. The numerical model showed to be suitable to study diverse phenomenon involved in free-breathing PEMFC performance.
© 2007 Elsevier B.V. All rights reserved.

Keywords: Free-breathing PEMFC; Modeling; Simulation; Current density distribution; Polymer electrolyte water content

1. Introduction

PEMFCs are usually operated under humidifying conditions around 80 °C to avoid dehydration of polymer electrolyte, reduce water condensation and increase reaction rate. Hence compressors, humidifiers and heaters are needed to achieve high and optimal power densities. Nevertheless, PEMFC may also be used for portable applications in which additional accessories like humidifiers and compressors cannot be utilized for practical reasons. Thus optimal performance of these applications directly depends on how species are supplied and disposed in the membrane and electrode assembly (MEA). Such applications are called "free-breathing" PEMFC provided that oxygen is taken from ambient air by diffusion and natural convection.

Performance of free-breathing PEMFC depends highly on natural convection and oxygen diffusion and so concentration losses become high in comparison to ohmic losses. The slow motion of reactants and oxygen diffusion are not the only factors that may cause high limiting effects, low convection may also result in a build up of water causing severe flooding at the cathode.

Even though concentration losses in cathode dominate free-breathing PEMFC performance, calculation of water content of polymer electrolyte and liquid saturation is necessary to establish a complete ohmic-concentration losses analysis. Previous experimental works concerning free-breathing PEMFC have been presented in Refs. [1–12]. Mennola et al. [8] presented both experimental and numerical data of oxygen and water mole fraction fields as well as velocity fields to provide insight of many details that may be important in understanding mass transport limiting controls in free-breathing PEMFC.

Given the small characteristic lengths in PEMFC, numerical modelling is important to provide insight into the different phenomenon and predict distributions that are difficult to be experimentally determined. Hence the objective of the present work is to carry out simulations to quantitatively analyze ohmic and concentration losses of free-breathing PEMFC power by using a non-isothermal and three-dimensional model [13] to account not only for natural convection and oxygen diffusion but also for water and heat management. Flow fields, energy and species transport, transport of water in polymer membrane and movement of liquid water in cathode and anode porous layers are determined under different hydrating conditions, cell temperatures, cathode catalyst loadings and channel lengths, in order to numerically determine limiting controls of free-breathing PEMFC.

* Corresponding author. Tel.: +49 921 557168; fax: +49 921 557165.
E-mail address: luis.matamoros@uni-bayreuth.de (L. Matamoros).

0378-7753/$ – see front matter © 2007 Elsevier B.V. All rights reserved.
doi:10.1016/j.jpowsour.2007.02.091

Nomenclature

ARH	anode relative humidity
C	molar concentration (kmol m^{-3})
CRH	ambient relative humidity
D	diffusivity (m^2 s^{-1})
F	Faraday constant
g	gravity acceleration (m s^{-2})
H	height (m)
K_p	hydraulic permeability (m^2)
LL	length (m)
M	molecular weight (kg kmol^{-1})
$\dot{n}_{GLH_2O}$	volumetric condensation rate (kg s^{-1} m^{-3})
N	molar flux (kmol m^{-2} s^{-1})
N_{drag}	electro-osmotic drag factor $(\mathrm{kmol_{H_2O}}(\mathrm{kmol_{H^+}})^{-1})$
P	pressure (Pa)
r	reaction rate (kmol s^{-1} m^{-3})
RH	relative humidity
s	saturation
S_ϕ	source term
T	temperature (K)
V	velocity (m s^{-1})

Greek letters

β	coefficient of volumetric expansion (K^{-1})
δ	thickness (m)
λ	water content $(\mathrm{kmol_{H_2O}}(\mathrm{kmol_{SO_3^-}})^{-1})$
μ	dynamic viscosity (kg m^{-1} s^{-1})
ϱ	density (kg m^{-3})

Subscripts

amb	ambient
c	capillary
CL	catalyst layer
GC	gas channel
GDL	gas diffusion layer
H^+	proton
H_2O	water
i	species i
im	immobile
L	liquid
m	mixture
O_2	oxygen
SO_3^-	sulfonate group
T	energy
V	momentum

2. Model description

As aforementioned, the model is three-dimensional and simultaneously calculates variables of gas channels, catalyst layers and polymer membrane in a vertical straight PEMFC with cathode gas channel ends open to ambient air. Fig. 1 shows geometrical characteristics of the control volume, which consists of a straight PEMFC. Anode inlet flow is assumed constant and in excess. Cathode inlet flow is assumed to be driven by buoyancy forces (natural convection). Membrane electrode assembly (MEA) comprises anode and cathode gas diffusion layers and catalyst layer as well as polymer membrane. Catalyst layers are assumed as an active volume; in order to account for proton resistance. Using a symmetry assumption, the domain was split in two parts and results for the left half were calculated. Details of modeling are presented in former work by our group [13].

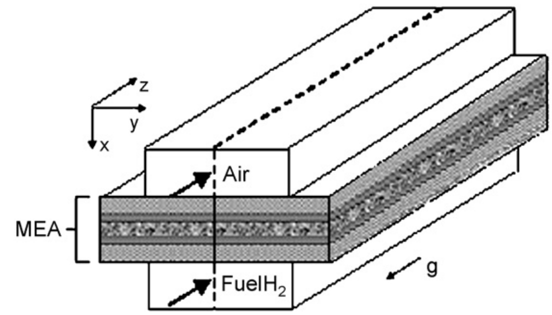

Fig. 1. Geometry of control volume.

2.1. Fundamental equations

Transport equations are simplified and expressed in general form:

$$V \cdot \nabla \varrho \phi = \nabla \Gamma \nabla \phi + S_\phi \tag{1}$$

where ϕ represents the variable to be calculated and Γ the diffusivity of this variable.

The continuity equation is represented by

$$\nabla \varrho V = S_m \tag{2}$$

Water content balance in polymer electrolyte is as follows:

$$\nabla D_\lambda \nabla \lambda = \frac{M_{SO_3^-}}{\varrho_{SO_3^-}} \frac{dN_{drag} N_{H^+}}{dx} \tag{3}$$

Liquid water balance in porous mediums can be expressed as

$$\nabla \frac{\varrho_{H_2O(L)} K_p S^3}{\mu_{H_2O(L)}} \left(\frac{dP_c}{dS}\right) \nabla S = \dot{n}_{GLH_2O} \tag{4}$$

where S represents the reduced saturation factor:

$$S = \frac{s - s_{im}}{1 - s_{im}} \tag{5}$$

2.2. Source terms

Natural convection is introduced in cathode gas channel momentum equation as source term (Eq. (6)). Diffusion is assumed to be the primary mechanism of transport in gas diffusion layers and catalyst layers. Pressure drop in anode gas channel (source term of momentum in anode gas channel) is estimated using Darcy friction factor, and so the use of coupled pressure–velocity equations is avoided. The source term of continuity equation (Eq. (2)) can be ignored [14].

$$S_V = \varrho\beta g(T - T_{amb}) \tag{6}$$

Joule heating in the polymer membrane, heat produced in cathode reaction and heat produced in condensation–evaporation entropy change are taken into account as source terms of energy S_T (Eqs. (7)–(9)). Joule heating S_{T1} in the membrane is calculated by using proton conductivity in Nafion k_{H^+} and proton flow as follows:

$$S_{T1} = \frac{(N_{H^+}F)^2}{k_{H^+}} \tag{7}$$

Heat produced by the reaction at the cathode is determined using reaction heat of oxygen reduction ΔHr_{O_2} and reaction rate:

$$S_{T2} = \Delta Hr_{O_2} r_{O_2} \tag{8}$$

And condensation–evaporation entropy change in cathode porous mediums is estimated using latent heat of vaporization of water at local temperature H_{LG} and volumetric condensation rate:

$$S_{T3} = H_{LG}\dot{n}_{GLH_2O} \tag{9}$$

Agglomerate model was used as electrochemical model [15–19]. The group of agglomerate model equations used in this work has been previously described in Ref. [13]. Electrochemical reaction rate obtained from agglomerate model is considered as source term of species S_i in catalyst layers:

$$S_i = M_i r_i \tag{10}$$

Stiochiometrical factors of every species are derived from the well-known mechanism of reaction in PEM fuel cells. Finally, condensation and evaporation processes in porous mediums are considered as an additional source term for the water to gas balance:

$$S_{H_2O} = \dot{n}_{GLH_2O} \tag{11}$$

2.3. Boundary conditions

In order to determine interfacial water transfer between cathode and anode porous mediums and the polymer membrane, the difference between bulk concentrations of water in each phase and equilibrium concentrations of water in the interface is used as the driving force of absorption and desorption of water by the polymer electrolyte. Convective mass transfer is neglected, and so water exchange is expressed in terms of molar fraction of each phase (Y_i and X_i) and mixture diffusivity of species i by each phase ($D_{i,m1}$ and $D_{i,m2}$):

$$\varrho_1 D_{i,m1}\frac{X_i - X_i^*}{M_1\Delta x_1} = \varrho_2 D_{i,m2}\frac{Y_i^* - Y_i}{M_2\Delta x_2} \tag{12}$$

The equilibrium data from Springer et al. [20] at 30 °C and from Hinatsu et al. [21] at 80 °C are used to complete this interfacial mass transfer model by relating the molar fraction of water of each phase at the interface (Y_i^* and X_i^*). It is important to mention that liquid water uptake from cathode and anode porous mediums is assumed as negligible.

Gas channel walls are assumed isothermal.

Table 1
Geometrical and electrochemical parameters

Description	Value
Channel height (m)	0.003
Channel width (m)	0.003
Channel length (m)	0.05
Channel rib (m)	0.0002
Gas diffusion layer thickness (m)	0.0001
Gas diffusion layer porosity	0.5
Catalyst layer thickness (m)	0.00001
Catalyst layer porosity	0.4
Polymer membrane thickness (m)	0.00023
Pt loading ($mg_{Pt}\,cm^{-2}$)	1.0
Pt surface area ($cm^2_{Pt}\,g_{Pt}{}^{-1}$)	250,000
Agglomerate porosity	0.2
Agglomerate radii (cm)	0.00001
Inlet anode volumetric flow ($m^3\,s^{-1}$)	0.0000001
Inlet cathode flow pressure (Pa)	101325.0
Inlet anode flow pressure (Pa)	300000.0
Ambient temperature (°C)	25

3. Results and discussion

Average current density and polymer membrane voltage loss along-channel distributions as well as average power density are presented as main output variables to study effects of operative conditions on free-breathing PEMFC performance. Simulations were carried out to observe influences of ambient and anode inlet flow relative humidity as well as cell temperature on free-breathing PEMFC power. Additionally, calculations using different cathode catalyst loadings and channel lengths were made to study concentration losses behavior when improving mass transfer and electrochemical conditions.

Even though modeling is non-isothermal, cell temperature is defined as an input variable. The input value that represents cell temperature is assumed equal to wall temperature, which is assumed constant as mentioned above. Such assumption showed to be suitable, given that temperature gradient can be neglected, basically due to small geometry and low current densities under free-breathing conditions. Moreover, inlet anode flow temperature is assumed equal to cell temperature, and so numerical results of temperature become almost uniform, even though cathode inlet flow temperature is constant in all calculations (25 °C).

Table 1 summarizes geometrical, electrochemical and operating parameters arbitrarily used in this work. Both current density and cell potential are considered output variables. Therefore, every input variable was kept constant except for the variable under study. As mentioned above, catalyst layers are assumed as an active volume, and so cathode overpotential becomes an output variable due to proton resistance. Hence, input cathode overpotential at the cathode catalyst layer–polymer membrane interface must be defined, in order to estimate ohmic losses in the cathode catalyst layer. This reference cathode overpotential

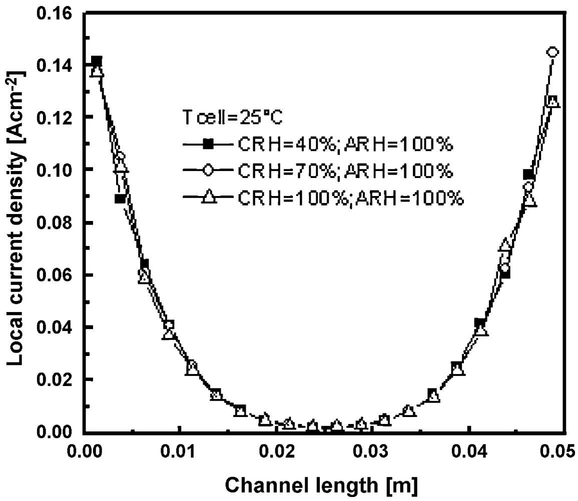

Fig. 2. Along channel current density for different ambient relative humidities at 25 °C.

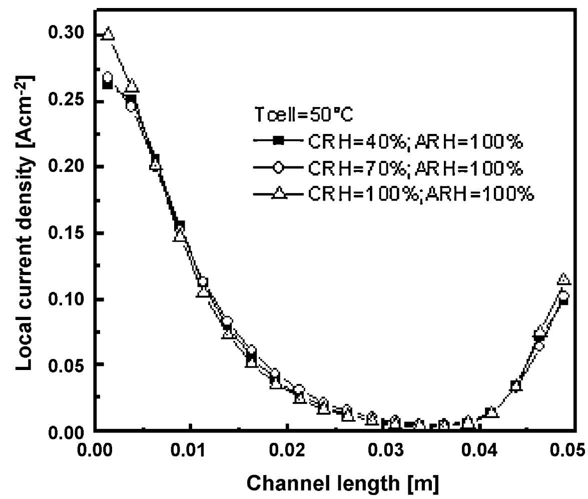

Fig. 3. Along channel current density for different ambient relative humidities at 50 °C.

is assumed constant (0.8 V under electrochemical conditions arbitrarily chosen in this work). Catalyst loading is assumed as 1.0 mg cm^{-2} and catalyst surface area as 250,000 cm^2 g^{-1}. Both values may provide relative good performance under free-breathing conditions, and so current density distributions may be suitable to study cell output under diverse conditions. It is important to mention that both values do not represent optimal electrode characteristics, because they were arbitrarily chosen. To analyze optimal electrode characteristics the relationship between catalyst loading and surface area should be defined in order to carry out numerical studies concerning catalyst loading in free-breathing PEMFC. Such task is not an objective of present work.

3.1. *Effect of humidity conditions*

As oxygen is directly taken from surrounding air, ambient conditions may have an influence on free-breathing PEMFC performance. Ambient relative humidity is taken as 40, 70 and 100% at 25 °C for different cell temperatures (25, 50 and 75 °C) while anode inlet flow is assumed to be fully humidified (100% ARH) at cell temperature.

Adjusting cell temperature at 25 °C (gas channel walls temperature), average power density is 0.585 V–0.0245 W cm^{-2}, 0.586 V–0.0251 W cm^{-2} and 0.586 V–0.0244 W cm^{-2} for 40, 70 and 100% air relative humidity, respectively. In this case oxygen supply is rather small, given that natural convection is negligible and diffusion through ends of cathode gas channel is the unique supply of oxidant for electrochemical reaction. Current density is rather low as a result of slow diffusion, and so cell potential is almost constant for every ambient relative humidity. As shown in Fig. 2, concentration losses highly dominate performance under these conditions, given that current density curves overlap for different ambient relative humidities. Therefore ambient relative humidity exerts a negligible effect on ohmic losses as result of low current densities yielded under such oxygen transfer control, and so power output is only governed by oxygen diffusion. Most of oxygen is consumed near ends of cathode gas channel and so average power density becomes low and highly controlled by oxidant transport. A considerable portion of the active area is barely used due to poor axial oxidant transport against through-plane diffusion and activation potential. Highest current densities at ends of cathode gas channel having almost symmetrical magnitudes are product of negligible convection and oxygen diffusion through boundaries.

At 50 °C of cell temperature, average power density is 0.567 V–0.0451 W cm^{-2}, 0.564 V–0.0454 W cm^{-2} and 0.569 V–0.0460 W cm^{-2} for 40, 70 and 100% air relative humidity, respectively. Considering that cell temperature is higher than ambient temperature, natural convection yields a smooth stream through cathode gas channel improving oxygen supply and as such the performance of the cell. The average inlet air velocity through gas channel is 0.017 m s^{-1}. As it can be observed in Fig. 3, highest current density is seen at entrance of gas channel. Oxygen is rapidly consumed by electrochemical reaction given the high activation potential needed to operate around 0.6 V. Presence of natural convection improves performance due to major availability and transport of oxidant in comparison to only-diffusion-driven-flux and then current density increases in comparison to former case (Fig. 2). Even though natural convection enhances oxygen supply, the cathode reaction seems to be highly controlled by concentration losses, given that cell potential is almost constant for every air relative humidity, which means that ohmic losses may be negligible under these conditions. At upper end of gas channel, oxygen counter-diffusion (against natural convection) yields a slight increment of current density as product of the short path between gas channel end boundary and active sites of cathode catalyst layer.

Increasing the cell temperature to 75 °C, average power density is 0.561 V–0.0633 W cm^{-2}, 0.561 V–0.0629 W cm^{-2} and 0.561 V–0.0625 W cm^{-2} for 40, 70 and 100% air relative humidity, respectively. Fig. 4(A) shows overlapping curves for different ambient relative humidities, which means that performance is even highly controlled by mass transport deficiencies over possible dehydration of polymer electrolyte. Nevertheless, current densities increase in comparison to former cases (25

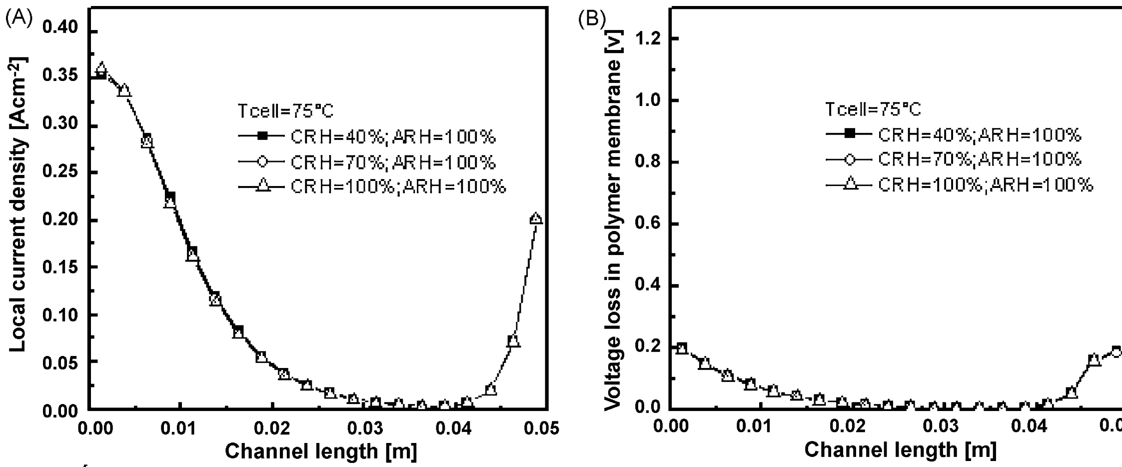

Fig. 4. (A) Along channel current density and (B) voltage loss in polymer membrane for different ambient relative humidities at 75 °C.

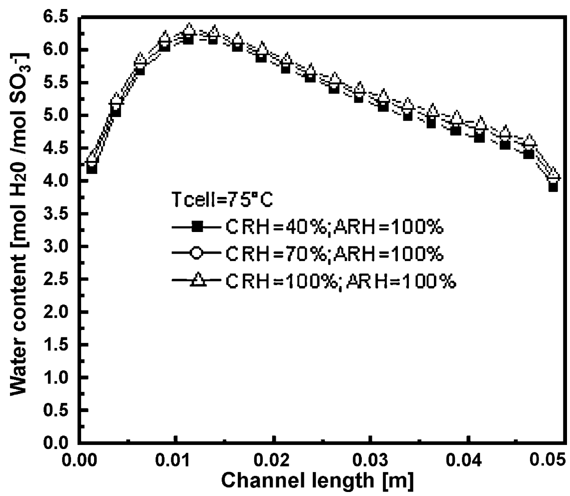

Fig. 5. Along channel average polymer membrane water content for different ambient relative humidities at 75 °C.

and 50 °C), basically due to increment of natural convective flow ($0.030\,\mathrm{m\,s^{-1}}$ average inlet air velocity) and oxygen diffusion. Not only natural convection and oxygen diffusion play an important role in electrochemical reaction but temperature does as well, given the increase of activation of cathode reaction by temperature. In this case, polymer membrane voltage loss is showed for different ambient relative humidities (Fig. 4(B)) in order to observe role of ohmic losses on cell performance under these conditions. It can be seen from Fig. 4(B) that voltage loss curves overlap for different ambient relative humidities, which means that ambient relative humidity may not affect cell output. Nonetheless, anode inlet flow relative humidity may have an important influence on hydration of polymer membrane provided that water content curves almost overlap for different ambient relative humidities (Fig. 5). Therefore fully humidifying conditions of anode inlet flow may reduce effect of ambient humidifying conditions on cell output by effectively hydrating polymer electrolyte. Hence the effect of anode inlet flow relative humidity becomes of importance when analyzing possible ohmic losses in free-breathing PEMFC. For this reason, anode inlet flow relative humidity was varied from 10 to 100% keeping ambient relative humidity at 70%, in order to observe performance of free-breathing PEMFC under such dehydrating conditions. As it can be seen in Fig. 6(A), anode inlet flow relative humidity may considerably affect cathode oxidation reaction by dehydrating the whole polymer electrolyte, and so increasing ohmic losses in cathode catalyst layer.

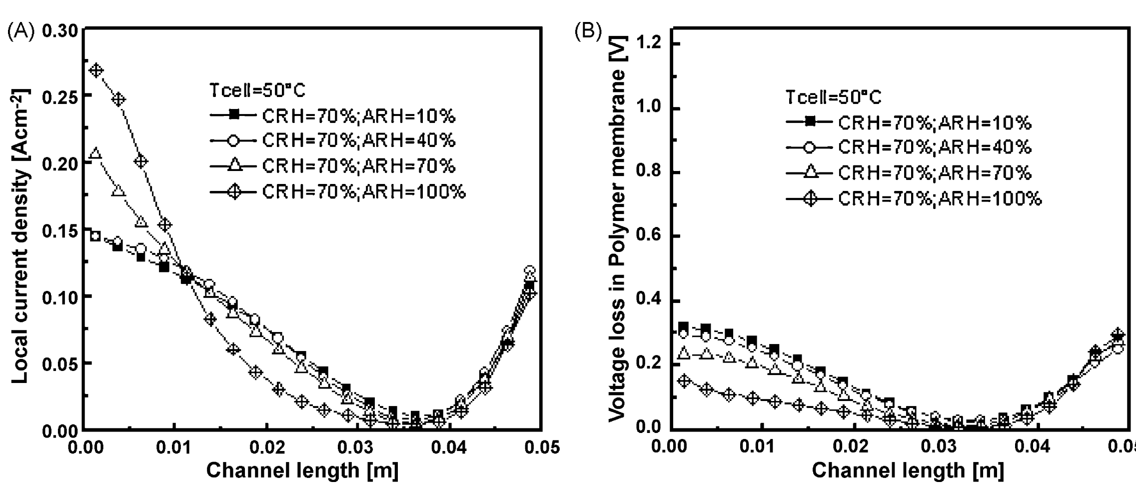

Fig. 6. (A) Along channel current density and (B) voltage loss in polymer membrane for different anode inlet flow relative humidities at 50 °C.

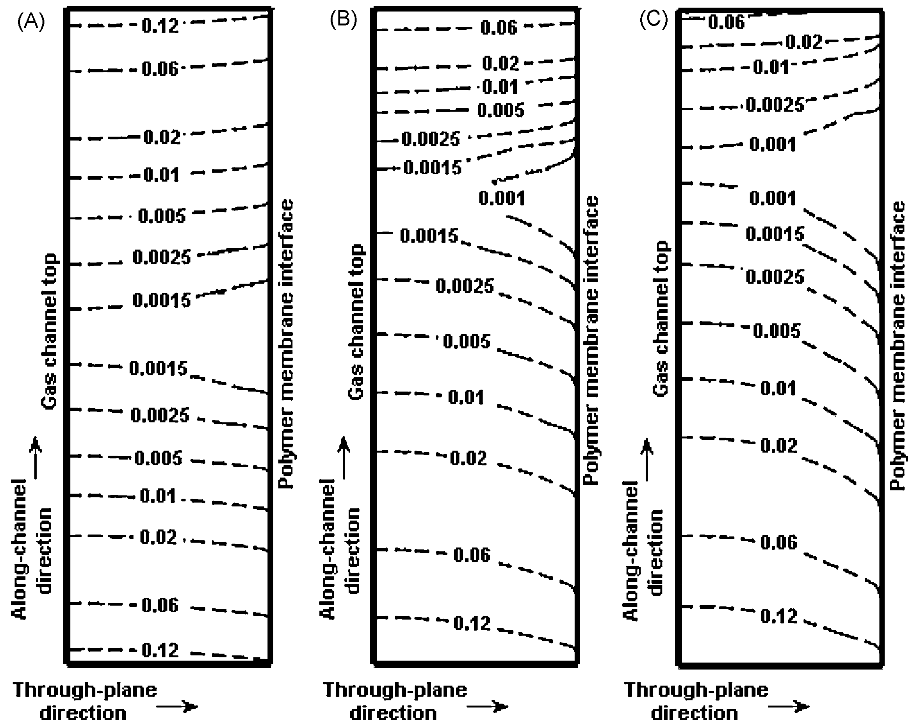

Fig. 7. Through-plane and along-channel oxygen mass fraction distributions at (A) 25, (B) 50 and (C) 75 °C.

Even though current density is relatively low, dehydration of polymer electrolyte may increase ohmic losses, consequently current density is affected at the entrance of gas channel by different anode inlet flow relative humidities (Fig. 6(A)). These differences decrease along gas channel due to depletion of oxygen and so irreversible local losses become minimal as product of low local current densities. This behavior can also be observed in polymer membrane voltage loss curves (Fig. 6(B)). Even though performance of free-breathing PEMFC may be slightly affected by such dehydrating conditions, concentration losses are definitely even more important. Average power density is 0.532 V–0.041 W cm^{-2}, 0.533 V–0.040 W cm^{-2}, 0.545 V–0.043 W cm^{-2} and 0.564 V–0.045 W cm^{-2} for 10, 40, 70 and 100% anode inlet relative humidity, respectively. Therefore, ohmic losses become slightly important when analyzing free-breathing PEMFC as long as local current densities are over 0.15 A cm^{-2} as it can be observed in Fig. 6(A) and (B).

3.2. Mass transport control

As mentioned above, oxygen supply is highly limiting in free-breathing PEMFC. Either with or without natural convection, oxygen transport to active sites seems to be rather poor as seen in former results. For this reason, estimation of oxygen concentration field are of high importance to illustrate limiting conditions to cathode electrochemical reaction. Fig. 7(A)–(C) shows along-channel and through-plane oxygen mass fraction maps using fully humidifying conditions at 25, 50 and 75 °C, respectively. The data aspect ratio was changed by reducing channel length aspect (1:5). Results show that through-plane oxygen transport is more effective in comparison to axial transport for all cases (25, 50 and 75 °C). Most of oxygen is consumed near gas channel ends given the more effective through-plane diffusion in comparison to axial convective and diffusive oxygen transport. Such behavior may be caused by differences in characteristic lengths for cathode mass transfer. Through-plane and axial characteristic lengths are around 0.003 and 0.05 m, respectively. Therefore short path of through-plane oxygen diffusion and activation of cathode reaction deplete oxygen rapidly and so a considerable portion of active sites may be barely used under these conditions given the relative long characteristic length for axial oxygen transport.

Lowest cell temperature (25 °C) and negligible natural convection considerably limit cell performance to low current densities as it can be seen in Fig. 7(A). Oxygen mass fraction is rapidly diminished at ends of gas channel from 0.23 to 0.12, given the high oxygen demand in this region. Afterwards axial diffusion of oxygen is rather slow; consequently oxygen mass fraction highly diminishes towards center of control volume. Fig. 7(B) shows that natural convection may enhance oxygen transport to active sites. Oxygen mass fraction is higher along gas channel entrance in comparison to Fig. 7(A), basically due to increase of natural convection. Consequently, oxygen depletion increases as a product of higher cathode reaction rate, which is stimulated by higher temperature and oxygen concentration. Therefore, the mass fraction map at 25 °C (Fig. 7(A)) is similar to the 50 °C map at the center of the cell (Fig. 7(B)). Towards the end of gas channel, natural convection dominates transport of oxygen over oxygen diffusion and so Fig. 7(B) shows a considerable decrease of oxygen fraction at upper end of gas channel in comparison to Fig. 7(A), given that upstream depleted oxygen flow is much higher than oxygen counter-diffusion, and so

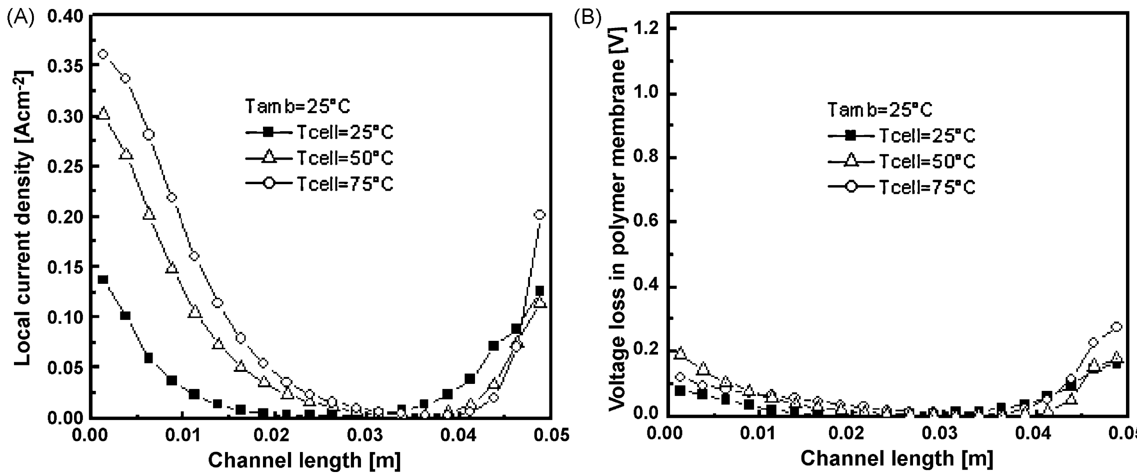

Fig. 8. (A) Along channel current density and (B) voltage loss in polymer membrane for different cell temperatures.

lower oxygen mass fraction is observed. Even so, performance of cell increases at higher temperatures. Fig. 7(C) showed to be similar to (B), even though temperature is higher, and so oxygen consumption. This effect is explained by former observation. Even though natural convection and diffusion are enhanced at 75 °C in comparison to 50 °C, cathode reaction rate is also higher and so oxygen depletion. As mentioned before, a lower oxygen fraction at upper end of gas channel (Fig. 7(B) and (C)) is a product of higher oxygen depleted upstream in comparison to counter-diffusion.

As seen cell temperature affects performance by increasing natural convection, oxygen diffusion and activation potential. Fig. 8(A) and (B) illustrate the role of temperature on cell output under fully humidifying conditions. Cell performance can considerably be increased using higher temperatures (A). Ohmic losses show a negligible effect on cell output (B), which means that concentration losses govern cell performance under free-breathing conditions.

Under such mass transport limitations, cathode catalyst loading may be an important parameter to observe. Fig. 9 shows current densities distribution for different cathode catalyst loadings (1.0, 2.5, 5.0 and 10 mg cm^{-2}). As it can be seen in Fig. 9, cathode catalyst loading enhances current density at gas channel ends. However this effect diminishes for higher catalyst loading, due to poor axial diffusion. Differences in current density distributions dramatically decrease along the gas channel, as result of depletion of oxygen which exclusively dominates performance over increase of active sites. Therefore increasing catalyst loading under such mass transfer controls may represent a high loss of cathode reaction efficiency.

Considering such limitations of axial oxygen transport, cell axial length is reduced to observe improvements in oxygen transport and overall performance. Results of Figs. 7–9 showed that cathode feed may be rather slow, and so free-breathing PEMFC performance is rather limited by rapid oxygen depletion at electrical potential around 0.6 V. Fig. 10 shows current density distributions using different channel lengths. As it can be seen, magnitudes of average current density are highly different due to shorter axial diffusion path, and so the active area becomes better utilized under chosen conditions. At end of gas channel, current density varies as product of upstream oxygen flow which is not

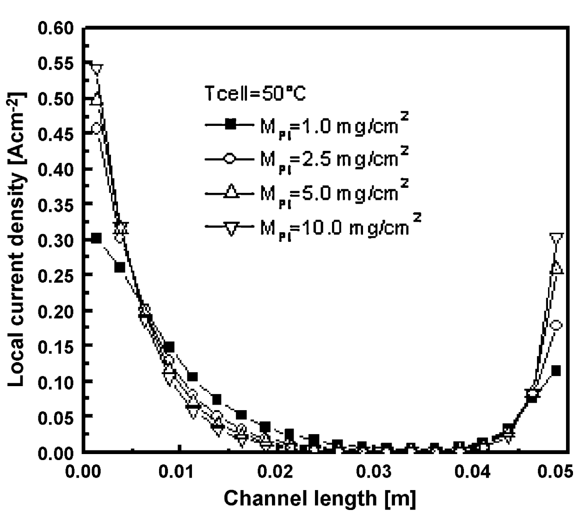

Fig. 9. Along channel current density using different cathode catalyst loadings at 50 °C.

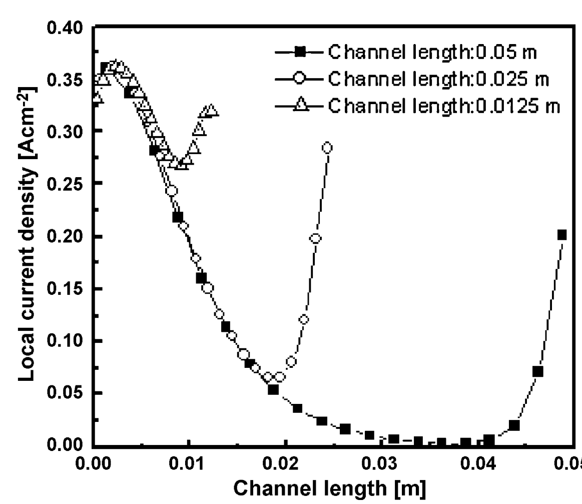

Fig. 10. Along channel current density using different channel lengths at 75 °C.

depleted for shorter gas channels. End current density is smallest for longest channel, given the depletion of oxygen upstream. However, once channel length is shorter, oxygen upstream and counter-diffusion yield higher current densities towards end of channel.

A simple approach can be made, in order to demonstrate role of natural convection over oxygen diffusion on concentration losses. Cathode reaction rate may be assumed as a first order mechanism, in order to simplify the analytic expression:

$$r_{O_2} = K_1 C_{O_2}^{CL}\, e^{-(K_2/T)} \tag{13}$$

where K_1 and K_2 represent cathode kinetic constants. Concentration of oxygen in cathode catalyst layer can be related to oxygen concentration at inlet as follows:

$$C_{O_2}^{CL} = \frac{C_{O_2\text{inlet}}}{[1 + K_1\, e^{-(K_2/T)}((\delta_{GDL}/D_{O_2,m}) + (LL_{GC}/H_{GC}V_{\text{inlet}}))]} \tag{14}$$

Terms that represent oxygen transport to active sites in former expression (Eq. (14)) are

$$\frac{\delta_{GDL}}{D_{O_2,m}} + \frac{LL_{GC}}{H_{GC}V_{\text{inlet}}} \tag{15}$$

Convective term (right) is around 1000 times higher than diffusive term (left) at 50 and 75 °C, which means that oxygen concentration in cathode catalyst layer is basically governed by behavior of natural convection under conditions of this work. Therefore, the role of temperature on oxygen diffusion may not be of importance when analyzing concentration losses, given that axial oxygen transport dominates free-breathing PEMFC performance.

4. Conclusions

Use of numerical tools is highly important to predict behaviors and distributions that are experimentally difficult to obtain. Therefore present work is useful to understand phenomenon concerning ohmic and concentration losses of free-breathing PEMFC power. Given the difficulties of obtaining experimental data to properly validate CFCD modeling and properties distributions, a simple comparison between *I–V* curves was made in former work [13] to ensure that this numerical modeling was suitable for studying ohmic and concentration losses. The authors in [13] mentioned that polarization curves are highly influenced by electrochemical reaction constants at low and moderate current densities and by ohmic and concentration losses at high current densities. A future goal is to compare experimental and numerical distributions to improve understanding of phenomenon that govern performance of PEMFC under different conditions. Wang [22] presented a detailed review of diverse works concerning measurements of current density distributions which may be used, together with numerical results, to yield an analysis concerning main limiting factors, in order to enhance understanding of processes involved in PEMFC.

In this work results showed that dehydrating conditions may yield considerable ohmic losses only if oxygen transport is high enough to produce average current densities over $0.15\ \mathrm{A\,cm^{-2}}$. Therefore use of fully humidified anode inlet flows would improve free-breathing PEMFC performance in case of operating at moderate current densities ($>0.15\ \mathrm{A\,cm^{-2}}$).

Concentration losses dominate free-breathing PEMFC performance. Axial oxygen transport constitutes main power loss, given that oxidant inlet flux is driven by natural convection and diffusion, which may be considered as slow transport mechanisms in comparison to forced convection. Therefore oxygen availability in active sites is highly limited and as such so current density.

Under conditions arbitrarily used to obtain numerical results, most of active area was barely utilized, given the unbalanced relation between axial transport of oxygen and activation of cathode reaction. Then considering such oxygen transport control, channel length constitutes an important parameter to account for, because most of reaction may take place at channel ends.

Considering high oxygen transport resistance in comparison to activation potential, only small amounts of cathode catalyst loadings are needed to yield acceptable free-breathing PEMFC performances.

References

[1] D. Chung, R. Jiang, J. Power Sources 83 (1999) 128–133.
[2] S. Morner, S.A. Klein, J. Solar Energy Eng. 123 (2001) 225–231.
[3] M. Noponen, T. Mennola, M. Mikkola, T. Hottinen, P. Lund, J. Power Sources 106 (2002) 304–312.
[4] M. Noponen, T. Hottinen, T. Mennola, M. Mikkola, P. Lund, J. Appl. Electrochem. 32 (2002) 1081–1089.
[5] T. Mennola, M. Mikkola, M. Noponen, T. Hottinen, P. Lund, J. Power Sources 112 (2002) 261–272.
[6] P.W. Li, T. Zhang, Q.M. Wang, L. Schaefer, M.K. Chyu, J. Power Sources 114 (2003) 63–69.
[7] T. Hottinen, M. Noponen, T. Mennola, O. Himanen, M. Mikkola, P. Lund, J. Appl. Electrochem. 33 (2003) 265–271.
[8] T. Mennola, M. Noponen, M. Aronniemi, T. Hottinen, M. Mikkola, O. Himanen, P. Lund, J. Appl. Electrochem. 33 (2003) 979–987.
[9] A. Schmitz, S. Wagner, R. Hahn, H. Uzun, C. Hebling, J. Power Sources 118 (2003) 162–171.
[10] T. Mennola, M. Noponen, T. Kallio, M. Mikkola, T. Hottinen, J. Appl. Electrochem. 34 (2004) 31–36.
[11] A. Schmitz, S. Wagner, R. Hahn, H. Uzun, C. Hebling, J. Power Sources 127 (2004) 197–205.
[12] T. Hottinen, M. Mikkola, P. Lund, J. Power Sources 129 (2004) 68–72.
[13] L. Matamoros, D. Brüggemann, J. Power Sources 161 (2006) 203–213.
[14] Y. Wang, C.-Y. Wang, J. Electrochem. Soc. 152 (2) (2005) A445–A453.
[15] K. Broka, P. Ekdunge, J. Appl. Electrochem. 27 (1997) 281–289.
[16] M.L. Perry, J. Newman, E.J. Cairns, J. Electrochem. Soc. 145 (1) (1998) 5–15.
[17] C. Marr, X. Li, J. Power Sources 77 (1999) 17–27.
[18] F. Jaouen, G. Lindbergh, G. Sundholm, J. Electrochem. Soc. 149 (4) (2002) A437–A447.
[19] Q. Wang, D. Song, T. Navessin, S. Holdcroft, Z. Liu, Electrochem. Acta 50 (2004) 725–730.
[20] T.E. Springer, T.A. Zawodzinski, S. Gottesfeld, J. Electrochem. Soc. 138 (8) (1991) 2334–2342.
[21] J.T. Hinatsu, M. Mizuhata, H. Takenata, J. Electrochem. Sources 141 (6) (1994) 1493–1498.
[22] C.-Y. Wang, Chem. Rev. 104 (10) (2004) 4727–4766.